Bifurcation in Dynamical Systems.
Deterministic Chaos. Quantum Chaos

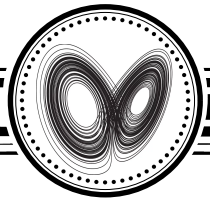

Izvestiya Vysshikh Uchebnykh Zavedeniy. Applied Nonlinear Dynamics. 2024;32(1)

Article DOI: 10.18500/0869-6632-003082

Parametric interaction of modes in the presence of quadratic or cubic nonlinearity

L.V. Turukina[1,2]

[1]Saratov Branch of Kotelnikov Institute of Radioengineering and Electronics of the RAS, Russia
[2]Saratov State University, Russia
E-mail: ✉turukinalv@yandex.ru

Received 28.04.2023, accepted 17.10.2023, available online 9.12.2023, published 31.01.2024

Abstract. *The purpose* of this work is a study of the dynamics of the systems of ordinary differential equations of the second order, which is obtained using the Lagrange formalism. These systems describe the parametric interaction of oscillators (modes) in the presence of a general quadratic or cubic nonlinearity. Also, we compare the dynamics of the systems of ordinary differential equations of the second order and dynamics of the Vyshkind –Rabinovich and Rabinovich–Fabrikant models in order to determine the possibilities of the latter models when modeling coupled oscillators of the above type. *Methods.* The study is based on the numerical solution using the methods of the theory of the obtained analytically differential equations. *Results.* For both systems of second-order differential equations, is was presented a chart of in the parameter plane, a graphs of Lyapunov exponents at the value of the parameter that specifies the dissipation of oscillators, a time dependences of the generalized coordinates of oscillators and its amplitudes, portraits of attractors, a projection of the attractors on a phase planes of oscillators. A comparison with the dynamics of the Vyshkind–Rabinovich and Rabinovich–Fabrikant models is carried out. These models are three-dimensional real approximations of the above systems obtained by the method of slowly varying amplitudes. *Conclusion.* The study of the constructed systems showed that in the parameter space there are regions corresponding to both various regular regimes, such as the equilibrium position, limit cycle, two-frequency tori, and chaotic regimes. For both systems, it was shown that the transition to chaos occurs as a result of a sequence of period doubling bifurcations of the tori. In addition, a comparison of the dynamics of the constructed systems with the dynamics of the Vyshkind– Rabinovich and Rabinovich–Fabrikant models allows us to assert that if the Vyshkind–Rabinovich model predicts the dynamics of the corresponding initial system well enough, then the Rabinovich–Fabrikant model does not have such a property.

Keywords: parametric interaction of the oscillators, chaotic attractors, Lagrange formalism, Lyapunov exponents.

Acknowledgements. Research was carried out under support of the Russian Science Foundation (project no. 21-12-00121), https://rscf.ru/project/21-12-00121/.

For citation: Turukina LV. Parametric interaction of modes in the presence of quadratic or cubic nonlinearity. Izvestiya VUZ. Applied Nonlinear Dynamics. 2024;32(1):11–30. DOI: 10.18500/0869-6632-003082

Introduction

Parametric interaction of wave or vibrational modes in nonlinear systems occurs in various fields of natural science [1–9]. A general model describing such interaction is a system called a resonant triplet, assuming that in a nonlinear system there is a weak interaction of three vibrational modes (the main mode and its two satellites), the frequencies of which satisfy the condition of parametric resonance. The simplest case refers to a degenerate parametric resonance, when the frequencies of the satellites are the same and the problem is reduced to considering the interaction of two vibrational modes. This assumption facilitates consideration and makes the analysis more understandable, since the dynamics depend on a smaller number of parameters.

One example of such systems is the Vyshkind-Rabinovich [8] and Rabinovich-Fabrikant [9] models proposed in the 70s of the last century. In the work [8] the authors considered the problem of weak interaction on the quadratic nonlinearity of three vibrational modes, the frequencies of which are subject to the parametric resonance condition $\omega_2 = \omega_1 + \omega_0$. Moreover, if in such a system a high-frequency mode is excited due to linear instability, and low-frequency modes are characterized by damping, then saturation of oscillations will be observed, determined by parametric decay. For the case of degenerate resonance, the authors of the work [8] obtained a model in the form of a system of three first-order differential equations:

$$\begin{aligned} \dot{x} &= z + \delta y - 2y^2 + \gamma x, \\ \dot{y} &= -\delta x + 2xy + \gamma y, \\ \dot{z} &= -2z(x+1). \end{aligned} \tag{1}$$

Here x, y, z are dynamic variables, and γ and δ are parameters. The works [8, 10] show that the dynamics of such a system can become chaotic, and the transition to chaos occurs through a sequence of bifurcations doubling the period of the limit cycle (Fig. 1, *a*).

The second model was obtained in the work [9]. In it, the authors considered the problem of modulation instability and the emergence of chaos during the parametric interaction of three modes in a nonequilibrium dissipative medium with cubic nonlinearity and a spectrally narrow gain. As for the previous model, in the case of degenerate resonance, the problem is reduced, under a number of simplifying assumptions, to a finite-dimensional system of differential equations for

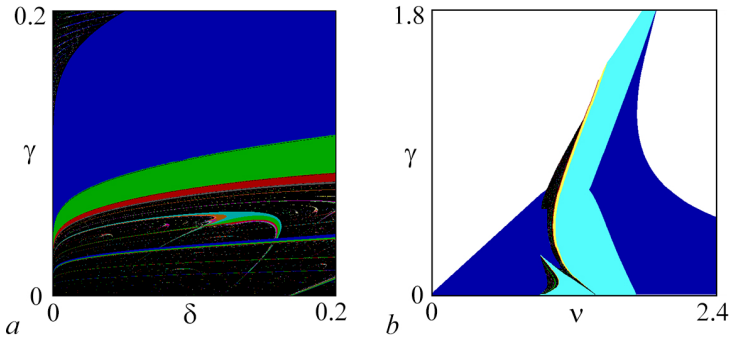

Fig 1. *a* — Chart of dynamical regimes of the Vyshkind–Rabinovich model (1) at (δ, γ) parameter plane. The chart taken from the work [10]. Blue color corresponds to the period one limit cycle, the green color correspond to the period two limit cycle, the red color correspond to the period four limit cycle, etc., the black color correspond to the chaos. *b* — Chart of dynamical regimes of the Rabinovich–Fabrikant model (2) at parameter plane (ν, γ). The chart taken from a work [18]. At the chart the blue color correspond to the equilibrium point, the light blue color correspond to the period one limit cycle, the yellow color correspond to the period two limit cycle, the red color correspond to the period four limit cycle, etc., the black color correspond to the chaos, the white color correspond to the regime when the trajectory go to infinity (color online)

three real variables

$$\begin{aligned}\dot{x} &= y(z-1+x^2)+\gamma x,\\ \dot{y} &= x(3z+1-x^2)+\gamma y,\\ \dot{z} &= -2z(\upsilon+xy),\end{aligned} \tag{2}$$

where x, y, z are dynamic variables, and γ and ν are parameters. Research in recent years has shown that the system (2) demonstrates quite rich dynamics: regular and chaotic attractors of different topologies, multistability, etc., and the transition to chaos, as for the previous model, occurs through a sequence of period doubling bifurcations limit cycle (Fig. 1, *b*) [11–20].

Note that the Vyshkind-Rabinovich (1) and Rabinovich–Fabrikant (2) models are universal in nature, since they describe systems of various physical natures, many of which have practical significance [1, 2, 6, 11, 21, 22].

Note, however, that both models were obtained under a number of simplifying assumptions for special cases of nonlinear equations with respect to complex amplitudes, which are generalizations of the well-known Landau model, and quadratic and cubic nonlinearities selected in a certain way. At the same time, in the work [19] the authors proposed a methodology based on the Lagrange mechanical formalism, which makes it possible to describe the parametric interaction of oscillators (oscillatory modes) in systems with a general nonlinearity using a system of ordinary differential equations (oscillator type) of the second order with respect to real variables. The idea of the method proposed in the work [19] is as follows. Let there be a system of oscillators described by the Lagrange equation:

$$\frac{d}{dt}\left(\frac{\partial L}{\partial \dot{x}_j}\right)-\frac{\partial L}{\partial x_j}=-\frac{\partial R}{\partial \dot{x}_j},\quad j=1,2,\ldots,N. \tag{3}$$

Here

$$L(x_1,x_2,\ldots,x_N)=\frac{1}{2}\sum_{n=1}^{N}(m_n\dot{x}_n^2-k_nx_n^2)-U(x_1,x_2,\ldots,x_N) \tag{4}$$

Lagrange function, and

$$R(x_1,x_1,\ldots,x_N)=\sum_{n=1}^{N}p_n\bar{\gamma}_n\dot{x}_n^2 \tag{5}$$

Rayleigh function, which determines the dissipation entering the system. The interaction potential $U(x_1,x_2,\ldots,x_N)$ is specified by a polynomial, the degree of which depends on what kind of nonlinearity is required and which is completely symmetric with respect to the permutation of oscillators. Then the Lagrange equations can be written as follows

$$\ddot{x}_j+2p_j\frac{\bar{\gamma}_j}{m_j}\dot{x}_j+\omega_j^2x_j+\frac{1}{m_j}\frac{\partial U}{\partial x_j}=0,\quad j=1,2,\ldots,N. \tag{6}$$

Here x_j are generalized coordinates of oscillators, $\bar{\gamma}_j$ are dissipation coefficients of oscillators, $\omega_j=\sqrt{k_j/m_j}$ — natural frequencies of oscillators, m_j — masses of oscillators. Note that the value p_n will take the following values: $p_n=-1$ if the dissipation coefficient is negative, and $p_n=1$ if it is positive. Obviously, the specific form of the system (6) will depend on the number of oscillators, the type of interaction potential, and the resonant condition imposed on the natural frequencies of the oscillators.

In this work, we study the simplest case—the parametric interaction of two oscillators (oscillatory modes). Two systems are considered. The first is a system of two (the main mode and its satellite) parametrically interacting oscillators in the presence of a general quadratic nonlinearity, and the second is in the presence of a general cubic nonlinearity. For both systems,

we choose the dissipation coefficients to be positive for the satellite and negative for the main mode. And the resonance conditions are respectively the same as for the Vyshkind-Rabinovich (case of quadratic nonlinearity) and Rabinovich-Fabrikant (case of cubic nonlinearity) models. The dynamics of both systems were studied numerically: in the space of selected parameters, regions of regular and chaotic dynamics were found and their transformation was studied when the remaining parameters included in the equations changed; the transition from regular to chaotic dynamics is described. A comparison of the obtained results with the results known for the Vyshkind-Rabinovich and Rabinovich-Fabrikant models was carried out in order to determine their capabilities and limitations when modeling coupled oscillators of the above type.

1. Parametric interaction of two oscillators in the case of general quadratic nonlinearity

First, let us consider the problem of the parametric interaction of two oscillators (oscillatory modes) in the presence of a general quadratic nonlinearity. In this case, we write the interaction potential $U(x_1, x_2, \ldots, x_N)$ in the following form:

$$U(x_1, x_2) = -\frac{1}{3}(x_1^3 + x_2^3) - \mu(x_1^2 x_2 + x_2^2 x_1), \tag{7}$$

where μ is a parameter characterizing the nonlinear interaction (nonlinearity parameter), and the Rayleigh function will be written as

$$R(x_1, x_2) = -\bar{\gamma}_1 \dot{x}_1^2 + \bar{\gamma}_2 \dot{x}_2^2. \tag{8}$$

Then the Lagrange equations (6) can be written explicitly as follows:

$$\begin{aligned} &\ddot{x}_1 + 2\frac{\bar{\gamma}_1}{m_1}\dot{x}_1 + \omega_1^2 x_1 - \frac{1}{m_1}(x_1^2 + 2\mu x_1 x_2 + \mu x_2^2) = 0, \\ &\ddot{x}_2 - 2\frac{\bar{\gamma}_2}{m_2}\dot{x}_2 + \omega_2^2 x_2 - \frac{1}{m_2}(x_2^2 + 2\mu x_1 x_2 + \mu x_1^2) = 0. \end{aligned} \tag{9}$$

Next, for convenience of research, we introduce new parameters. Namely $\gamma_j = \bar{\gamma}_j / m_j$ — dissipation parameter and $\alpha_j = 1/m_j$ — nonlinear interaction parameter. Then the system (9) will take the form:

$$\begin{aligned} &\ddot{x}_1 + 2\gamma_1 \dot{x}_1 + \omega_1^2 x_1 - \alpha_1(x_1^2 + 2\mu x_1 x_2 + \mu x_2^2) = 0, \\ &\ddot{x}_2 - 2\gamma_2 \dot{x}_2 + \omega_2^2 x_2 - \alpha_2(x_2^2 + 2\mu x_1 x_2 + \mu x_1^2) = 0. \end{aligned} \tag{10}$$

Here the main mode corresponds to the oscillator with the index 2, and the satellite corresponds to the index 1. Note that in what follows we will study the system (10), which we will call the original system.

Let the resonance condition have the form $\omega_2 \approx 2\omega_1$. Then, assuming that nonlinearity and dissipation are small, that is, the amplitudes of the oscillators change slightly over a characteristic time interval, we apply the method of slow amplitudes to the system (10). To do this, let us represent the generalized coordinates of the oscillators in the form

$$\begin{aligned} x_1 &= A_1 e^{i\omega_1 t} + A_1^* e^{-i\omega_1 t}, \\ x_2 &= A_2 e^{i\omega t} + A_2^* e^{-i\omega t}, \end{aligned} \tag{11}$$

and impose an additional condition

$$\begin{aligned} &\dot{A}_1 e^{i\omega_1 t} - \dot{A}_1^* e^{-i\omega_1 t} = 0, \\ &\dot{A}_2 e^{i\omega t} - \dot{A}_2^* e^{-i\omega t} = 0, \end{aligned} \tag{12}$$

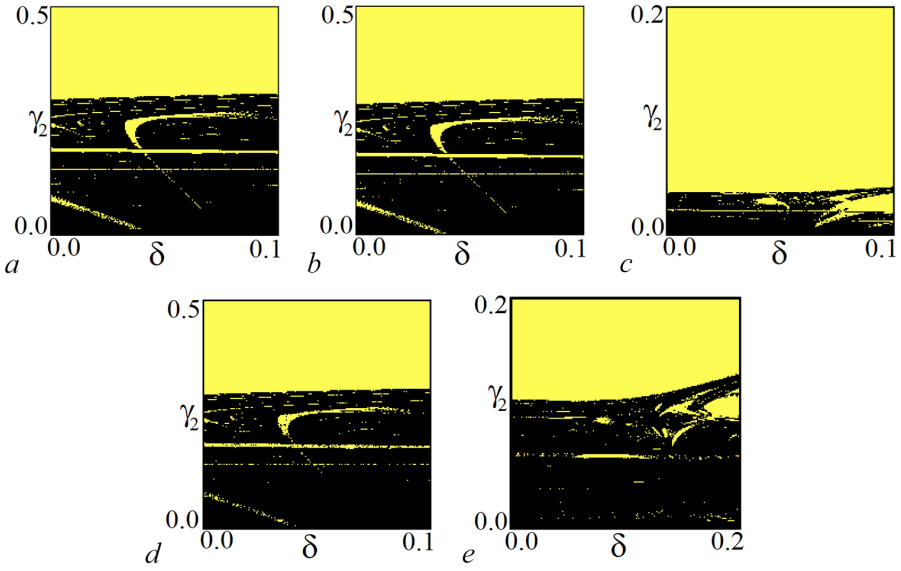

Fig 2. Charts of Lyapunov exponents of the system (10) and its enlarged fragment at (δ, γ_2) parameter plane. *a* — $\omega_1 = 6\pi$, $\omega_2 = 2\omega_1 - \delta$, $\gamma_1 = 1$, $\mu = 1$, $\alpha_1 = 1$, $\alpha_2 = 1$; *b* — $\omega_1 = 6\pi$, $\omega_2 = 2\omega_1 - \delta$, $\gamma_1 = 0.25$, $\mu = 1$, $\alpha_1 = 1$, $\alpha_2 = 1$; *c* — $\omega_1 = 6\pi$, $\omega_2 = 2\omega_1 - \delta$, $\gamma_1 = 1$, $\mu = 0.25$, $\alpha_1 = 1$, $\alpha_2 = 1$; *d* — $\omega_1 = 6\pi$, $\omega_2 = 2\omega_1 - \delta$, $\gamma_1 = 1$, $\mu = 1$, $\alpha_1 = 1$, $\alpha_2 = 0.5$; *e* — $\omega_1 = 60\pi$, $\omega_2 = 2\omega_1 - \delta$, $\gamma_1 = 1$, $\mu = 1$, $\alpha_1 = 1$, $\alpha_2 = 1$ (color online)

where A_j are the complex amplitudes of the oscillators, and $\omega = 2\omega_1$.

After substituting expressions (11), (12) into equations (10), averaging over time and bringing similar terms for new complex amplitudes a_j, where

$$\begin{aligned} a_1 &= \frac{\mu\sqrt{\alpha_1\alpha_2}}{2\omega_1} A_1, \\ a_2 &= \frac{\mu\alpha_1}{\omega_1} A_2, \end{aligned} \tag{13}$$

we obtain the following amplitude equations:

$$\begin{aligned} \dot{a}_1 + 2\gamma_1 a_1 &= -i a_1^* a_2, \\ \dot{a}_2 - 2\gamma_2 a_2 - i\delta a_2 &= -i a_1^2, \end{aligned} \tag{14}$$

where $\delta = \omega_1 - \omega = \omega_2 - 2\omega_1$ — frequency detuning from resonance. Note that the system (14) coincides with a similar system obtained in the works [8, 10], which, when moving to real amplitudes and phases, is reduced to the Vyshkind–Rabinovich model (1), if we put $\gamma_1 = 1$, $\gamma_2 = \gamma$, $\delta = -\delta$. It is obvious that for the system (14), acting similarly to the works [8, 10], it is possible to obtain a modification of the Vyshkind–Rabinovich model (1), in which the parameter γ_1. However, as will be shown below, the influence of the dissipation parameter γ_1 on the dynamics of the system (10) consists only of rescaling the parameter plane. Therefore, in this work we will limit ourselves to only studying the dynamics of the system (10).

Now let us study the dynamics of the system (10). To begin with, let's construct maps of Lyapunov exponents for it on the parameter plane (δ, γ_2) (Fig. 2). They were built as follows. At each point of the plane, four (full spectrum) Lyapunov exponents were numerically calculated[1], as

[1]The equality of Lyapunov exponents to zero was checked with an accuracy of tolerance, the value of which was 10^{-4}; the accuracy of calculating the indices themselves was about 10^{-5} . The calculation time for the indicators was 10^7. It should be noted that the appearance of maps on the parameter plane does not change significantly with increasing duration and accuracy of calculations.

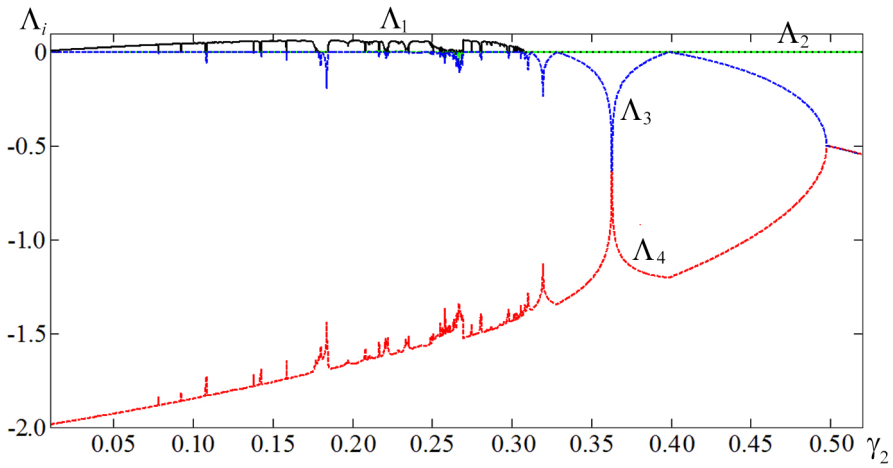

Fig 3. Graphs of Lyapunov exponents of the system (10) at the value of the parameter γ_2. $\omega_1 = 6\pi$, $\omega_2 = 2\omega_1 - \delta$, $\gamma_1 = 1$, $\mu = 1$, $\alpha_1 = 1$, $\alpha_2 = 1$, $\delta = 0.08$ (color online)

was done, for example, in the works [23–25]. After which the point was painted in a certain color depending on the signature of the indicators. The maps presented in Fig. 2 use the following color palette: yellow color corresponds to a two-frequency torus, when the first and second indicators are zero, and the third and fourth are negative; black color corresponds to the chaotic mode — the highest indicator is positive, the second and third are zero, and the fourth is negative.

Fig. 2, *a* shows the map of indicators of the Lyapunov system (10), constructed for the following parameter values $\omega_1 = 6\pi$, $\omega_2 = 2\omega_1 - \delta$, $\gamma_1 = 1$, $\mu = 1$, $\alpha_1 = 1$, $\alpha_2 = 1$, that is, for the case when the system (14) completely coincides with a similar system obtained in the works [8, 10]. In other words, this is the case where the Vyshkind–Rabinovich model (1) can be considered as a three-dimensional real approximation of the original system (10). Accordingly, one can compare their dynamics. From a comparison of Fig. 2, *a* and Fig. 1, *a* it is clear that, up to a scale transformation along the axes, very good correspondence. Namely, in the upper part of both maps there are areas of regular dynamics. In the case of the Vyshkind–Rabinovich model (1) these are limit cycles of various periods, and in the case of the system (10) these are two-frequency tori. In the lower part of both maps, areas of chaotic dynamics are observed, within which there are areas of regular dynamics. It is easy to show that as the parameter γ_2 decreases in the system (10), similarly to the Vyshkind–Rabinovich model (1), a transition to chaos will be observed through a sequence of period doubling bifurcations, only Now it is not the limit cycles that will double, but the tori. To show this, for the system (10) we plot the dependence of the Lyapunov exponents on the parameter γ_2 at a fixed value of the parameter $\delta = 0.08$. The corresponding graph is presented in Fig. 3.

From Fig. 3 it is clear that for parameter values $\gamma_2 > 0.31$ the first and second indicators are zero, and the third and fourth are negative, which corresponds to a dynamic regime in the form of a two-frequency torus. In this case, the change in the value of the third exponent with decreasing parameter γ_2 is typical for systems in which there is a transition to chaos through a sequence of period doubling bifurcations [26]. Namely, its value first decreases in absolute value until it touches the axis $\Lambda_j = 0$, then increases, etc. In Fig. 4, *a*, textitb presents the time dependences of the generalized coordinates of the oscillators x_1 and x_2 (left column), as well as the values of $|a_1|$ and $|a_2|$ (middle column) for a torus of period one (Fig. 4, *a*) and a torus of period two (Fig. 4, *b*). The Lyapunov exponents are respectively $\Lambda_1 = 0.00000 \pm 0.00001$, $\Lambda_2 = 0.00000 \pm 0.00001$, $\Lambda_3 = -0.11171 \pm 0.00001$, $\Lambda_4 = -0.98831 \pm 0.00001$ and $\Lambda_1 = 0.00000 \pm 0.00001$, $\Lambda_2 = 0.00000 \pm 0.00001$, $\Lambda_3 = -0.09324 \pm 0.00001$, $\Lambda_4 = -1.20678 \pm 0.00001$.

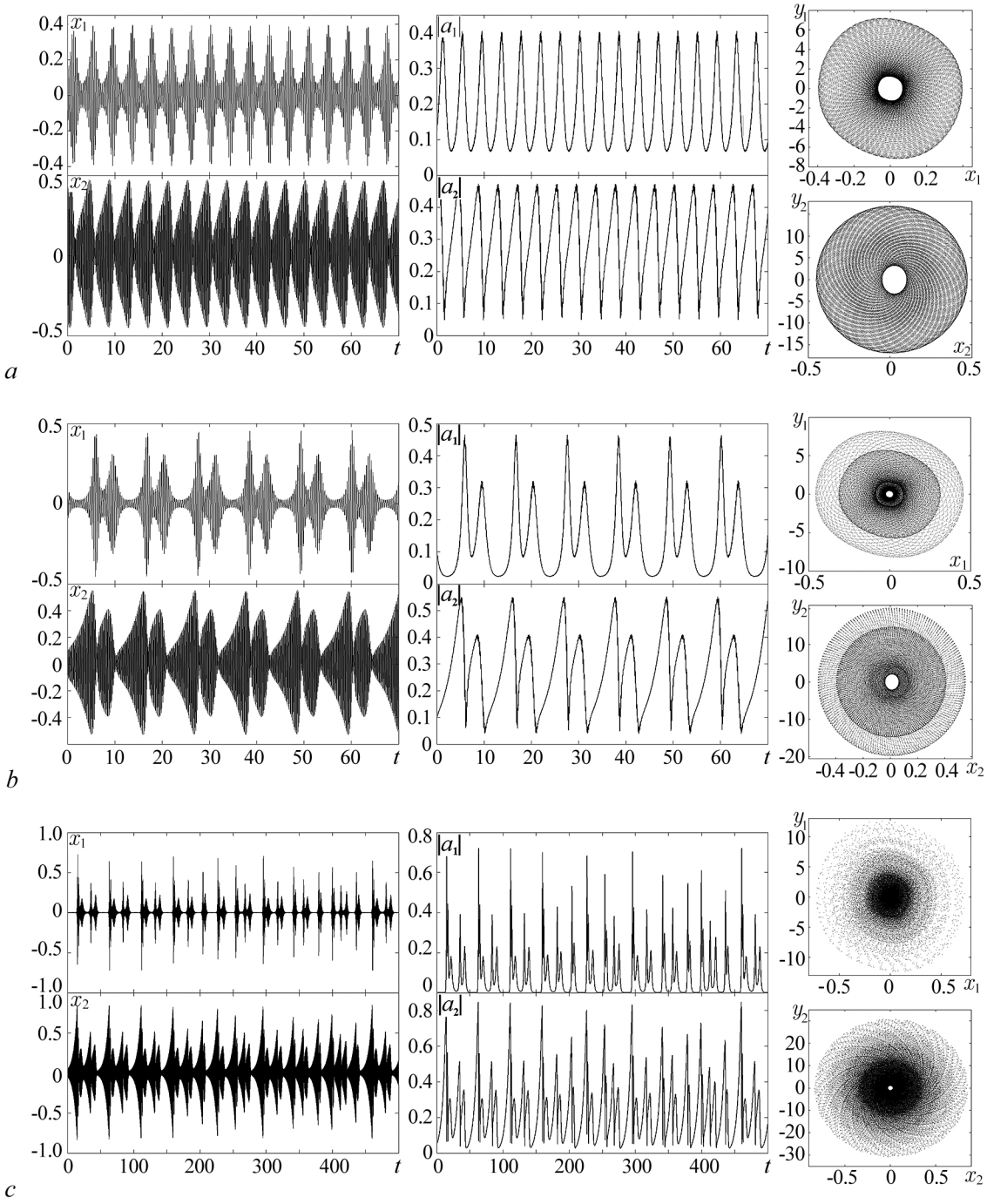

Fig 4. At the left column present the time dependencies of the generalized coordinates of oscillators x_1, x_2 of the system (10). At the middle column present the time dependencies of the $|a_1|$, $|a_2|$ of the system (10). At the right column present the projection of the attractors on a (x_1, y_1) and (x_2, y_2) plane of the system (10). *a* — The two-frequency period one torus, $\gamma_2 = 0.45$; *b* — the two-frequency period two torus, $\gamma_2 = 0.35$; *c* — the chaos, $\gamma_2 = 0.2$. Other parameters are $\omega_1 = 6\pi$, $\omega_2 = 2\omega_1 - \delta$, $\delta = 0.08$, $\gamma_1 = 1$, $\mu = 1$, $\alpha_1 = 1$, $\alpha_2 = 1$

With a further decrease in the parameter γ_2, the leading Lyapunov exponent becomes positive and a chaotic regime is observed in the system (10). The corresponding time dependences of the generalized coordinates of the oscillators x_1 and x_2 (left column) and the quantities $|a_1|$ and $|a_2|$ (middle column) are presented in Fig. 4, *c*, and the Lyapunov exponents have the values $\Lambda_1 = = 0.06233 \pm 0.00001$, $\Lambda_2 = 0.00000 \pm 0.00001$, $\Lambda_3 = 0.00000 \pm 0.00001$, $\Lambda_4 = -1.66311 \pm 0.00001$. Note that all temporary implementations in Fig. 4 demonstrate behavior typical for the presented modes.

The right column of Fig. 4 shows the projections of the corresponding attractors of the system (10) on the plane of generalized coordinates of the first and second oscillators. Thus, in Fig. 4, *a* an attractor is presented in the form of a torus of period one, in Fig. 4, *b* — an attractor in the form of a torus of period two, and in Fig. 4, *c* — a chaotic attractor. Note that the ranges of changes in the generalized velocities of the oscillators y_1, y_2 and the generalized coordinates of the oscillators x_1, x_2 differ by an order of magnitude. Also, the projections of attractors corresponding to tori, regardless of their period, have a clearly defined internal structure, but a chaotic attractor does not have such a structure.

Note that the system (10) contains a fairly large number of parameters, so the next step in the study is obviously to analyze how changing these parameters affects its dynamics. First, let us change the dissipation parameter γ_1. The corresponding map of Lyapunov system exponents (10) is presented in Fig. 2, *b*. From a comparison of this figure with Fig. 2, *a* it is clear that the dissipation parameter γ_1 plays the role of a scale factor. Reducing it causes the map to shrink along both axes. As a result, the transition from regular to chaotic regimes occurs at significantly lower values of the parameter γ_2, and in the chaos region on the right, new structures corresponding to regular regimes appear (compare Fig. 2, textita and 2, *c*).

Now let us consider how the dynamics of the system (10) are influenced by the parameters characterizing the nonlinear interaction. Namely, the parameters μ and $\alpha_{1,2}$. Fig. 2, *c* shows the map of Lyapunov system exponents (10), constructed for $\mu = 0.25$. From a comparison of Fig. 2, *a* and 2, *c* it is clear that the maps constructed for $\mu = 1$ and $\mu = 0.25$ look almost identical, demonstrating only a slight downward shift in the transition boundary from regular to chaotic regimes. Note, however, that at $\mu = 0$ the system (10) turns into a system of two uncoupled oscillators. In this case, the dissipation of the first oscillator is positive, and the dissipation of the second is negative, that is, the oscillations of the first oscillator will decay, and the second will increase indefinitely (run away to infinity). In the case of $\mu \neq 0$, even if μ is very small, there will be parametric interaction between the oscillators in the system (10). This will lead to an exchange of energy between the oscillators and when the parameter μ exceeds a certain threshold value in the system, saturation of oscillations will be observed. Fig. 5 shows the dependence graphs of the functions $U_1 = x_1^2 + 2\mu x_1 x_2 + \mu x_2^2$ and $U_2 = x_2^2 + 2\mu x_1 x_2 + \mu x_1^2$ from the parameter μ, illustrating this process . The graphs are plotted for the following parameter values: $\omega_1 = 6\pi$, $\omega_2 = 2\omega_1 - \delta$, $\delta = 0.08$, $\gamma_1 = 1$, $\gamma_2 = 0.45$, $\alpha_1 = 1$, $\alpha_2 = 1$. The figure shows that for $\mu = 0$, $U_1 = 0$, and $U_2 \to \infty$. As μ increases, U_1 increases, and U_2 decreases, and at $\mu \approx 0.16$ their values become the same. If we continue to increase the parameter μ, then the values of U_1 and U_2, although they change slightly, will remain close. Thus, the μ parameter is responsible for establishing oscillation saturation in the system (10). As soon as this happens ($\mu > 0.16$), the parameter μ weakly, especially in comparison with, for example, the dissipation parameter, affects the dynamics of the system under consideration. Therefore, all studies of the system (10) were carried out in that region of the parameter space where saturation of oscillations was established.

And finally, let us change the frequency of the first oscillator ω_1, increasing it tenfold.

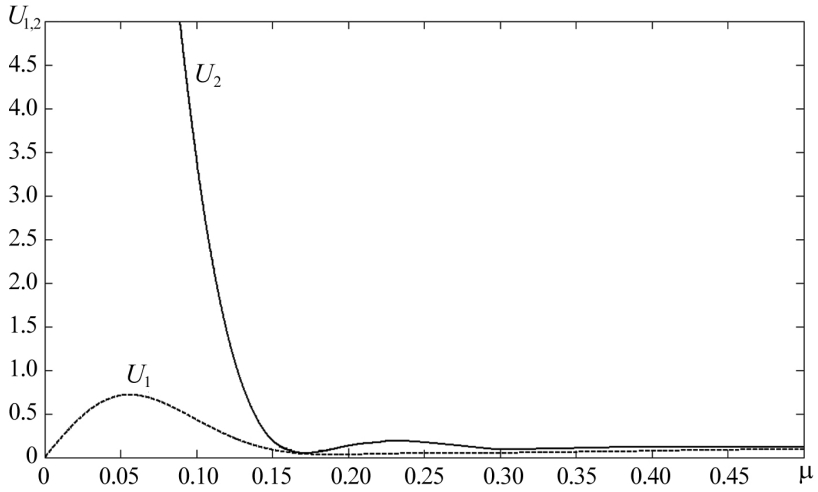

Fig 5. Graphs of the functions $U_{1,2}$ at the value of the parameter μ. $\omega_1 = 6\pi$, $\omega_2 = 2\omega_1 - \delta$, $\delta = 0.08$, $\gamma_1 = 1$, $\gamma_2 = 0.45$, $\alpha_1 = 1$, $\alpha_2 = 1$

The corresponding map of Lyapunov system exponents (10) is presented in Fig. 2, *e*. From a comparison of the figures (see Fig. 2, *a* and Fig. 2, *e*) it is clear that the increase in the frequencies of the first oscillator, as well as and changing the dissipation parameter leads to a large-scale transformation of the map: the observed picture of areas of regular and chaotic regimes is compressed along the axes. As a consequence, the transition from regular regimes to chaos occurs at lower values of the parameter γ_2.

In conclusion of this part, we note that not all terms included in the interaction potential $U(x_1, x_2)$ are resonant and contribute to the amplitude equations (14). However, if in the equations of the system (10) we leave only resonant terms, namely $2\mu x_1 x_2$ in the first equation and μx_1^2 in the second , then the dynamics of the system (10) will remain virtually unchanged: again, only a large-scale transformation of the parameter space will take place. Therefore, it can be argued that the non-resonant terms included in the interaction potential $U(x_1, x_2)$ have little effect on the dynamics of the system (10).

2. Parametric interaction of two oscillators in the case of cubic nonlinearity of general form

Now let us consider the problem of the parametric interaction of two oscillators (oscillatory modes) in the presence of a cubic nonlinearity of a general form. In this case, the interaction potential $U(x_0, x_1)$ will take the following form:

$$U(x_0, x_1) = \frac{1}{4}\left(x_0^4 + x_1^4\right) + \beta\left(x_0^3 x_1 + x_1^3 x_0\right) + \frac{3}{2}\mu x_1^2 x_1^2. \tag{15}$$

Here μ, β are parameters characterizing nonlinear interaction (nonlinearity parameters). In turn, we write the Rayleigh function in the form:

$$R(x_0, x_1) = \frac{1}{2}\left(\bar{\gamma}_0 \dot{x}_0^2 - \bar{\gamma}_1 \dot{x}_1^2\right). \tag{16}$$

Then the Lagrange equations (6) take the form

$$\begin{aligned} &\ddot{x}_0 - \gamma_0 \dot{x}_0 + \omega_0^2 x_0 + \alpha_0\left(x_0^3 + \beta(3x_0^2 x_1 + x_1^3) + 3\mu x_0 x_1^2\right) = 0, \\ &\ddot{x}_1 + \gamma_1 \dot{x}_1 + \omega_1^2 x_1 + \alpha_1\left(x_1^3 + \beta(3x_1^2 x_0 + x_0^3) + 3\mu x_1 x_0^2\right) = 0. \end{aligned} \tag{17}$$

Here, as in the previous section, new parameters are introduced: $\gamma_j = \bar{\gamma}_j/m_j$ — dissipation parameter and $\alpha_j = 1/m_j$ — nonlinear interaction parameter. In this case, the main mode corresponds to the oscillator with the index 0, and the satellite corresponds to the index 1. Note that in what follows the system (17) will be called the original system.

Let the resonance condition have the form $\omega_0 \approx \omega_1$. Then, similarly to the previous section, under the assumption of low nonlinearity and dissipation, we apply the method of slow amplitudes to the system (17), representing the generalized coordinates of the oscillators in the form

$$\begin{aligned} x_0 &= a_0 e^{i\omega_0 t} + a_0^* e^{-i\omega_0 t}, \\ x_1 &= a_1 e^{i\omega_1 t} + a_1^* e^{-i\omega_1 t}, \end{aligned} \tag{18}$$

and imposing an additional condition

$$\begin{aligned} &\dot{a}_0 e^{i\omega_0 t} - \dot{a}_0^* e^{-i\omega_0 t}, \\ &\dot{a}_1 e^{i\omega_1 t} - \dot{a}_1^* e^{-i\omega_1 t}, \end{aligned} \tag{19}$$

where a_j are the complex amplitudes of the oscillators.

Let us substitute the expressions (18), (19) into the equations (17). Proceeding similarly to the works of [9,19], after averaging over time and reducing similar terms, taking into account possible frequency deviation from resonance $\Delta\omega = \omega_0 - \omega_1 \neq 0$ in exponent, we obtain the following equations for complex amplitudes:

$$\begin{aligned} \dot{a}_0 &= \frac{1}{2}\gamma_0 a_0 + i\frac{3}{2\omega_0 m_0}\left[\mu a_0^* a_1^2 e^{-2i\Delta\omega t} + \left(|a_0|^2 + 2\mu|a_1|^2\right) a_0\right], \\ \dot{a}_1 &= -\frac{1}{2}\gamma_1 a_1 + i\frac{3}{2\omega_1 m_1}\left[\mu a_1^* a_0^2 e^{i\Delta\omega t} + \left(|a_1|^2 + 2\mu|a_0|^2\right) a_1\right]. \end{aligned} \tag{20}$$

Note that the system (20), up to changing the coefficients in front of the terms, is similar to the system obtained in the work [19][2], which, when moving to real amplitudes and phases is reduced to the Rabinovich–Fabrikant model (2) under the condition $\mu = 1$. The dynamics of the latter were studied in detail in the works [18–20].

As in the previous section, we begin the study of the dynamics of the system (17) by constructing maps of Lyapunov exponents. The corresponding maps and their enlarged fragments, built on the plane (γ_0, γ_1), are presented in Fig. 6. These maps use the following color palette: blue color corresponds to the equilibrium position — all indicators are negative; blue color corresponds to the periodic mode (limit cycle) — one zero indicator; yellow color corresponds to the quasiperiodic mode (dual-frequency torus) — two zero indicators; black color corresponds to the chaotic mode — at least one positive indicator, and white color corresponds to the trajectory running away to infinity.

Fig. 6, *a* shows the map and its enlarged fragments, built for the following parameter values: $\omega_0 = 32\pi$, $\omega_1 = \omega_0 - 1$, $\mu = 8$, $\beta = 2$, $\alpha_0 = 1$, $\alpha_1 = 1$. The figure shows that in the lower right part of the map (region $\gamma_0 < 1.29$ and $\gamma_1 > -1.22$, blue region) the system exhibits

[2]Note that in the work [19] a system of three coupled oscillators was considered — the main mode and its two satellites. Accordingly, the interaction potential contained a larger number of terms and parameters. As a result, for complex amplitudes a three-dimensional system was also obtained, containing a larger number of terms and parameters. As a result, to derive the Rabinovich-Fabrikant model, a transition was made to the two-dimensional case under the assumption that the amplitudes and parameters, such as dissipation and frequency, of the satellites coincide. Therefore, strictly speaking, the system (20) and the system of amplitude equations obtained in the work [19] are slightly different models that coincide when replacing parameters and reducing similar terms.

a regime in the form of a trivial equilibrium position. This is confirmed by the graphs of the dependence of the Lyapunov exponent of the system (17) on the parameters γ_0 and γ_1, presented in Fig. 7. It is clear from them that in this region all four Lyapunov exponents are negative.

When leaving the region of existence of a trivial equilibrium position through the upper (increase the parameter γ_0) or left (decreasing the parameter γ_1) boundaries, the equilibrium position becomes unstable and a limit cycle is born in the system. On the graphs of the dependence of the Lyapunov exponents on the parameters γ_0 and γ_1 (Fig. 7), this corresponds to the fact that the highest Lyapunov exponent becomes equal to zero, while all the others indicators continue to remain negative. The corresponding projections of the attractor onto the phase planes of the oscillators are presented in Fig. 8, *a* and represent highly elongated ellipses, since

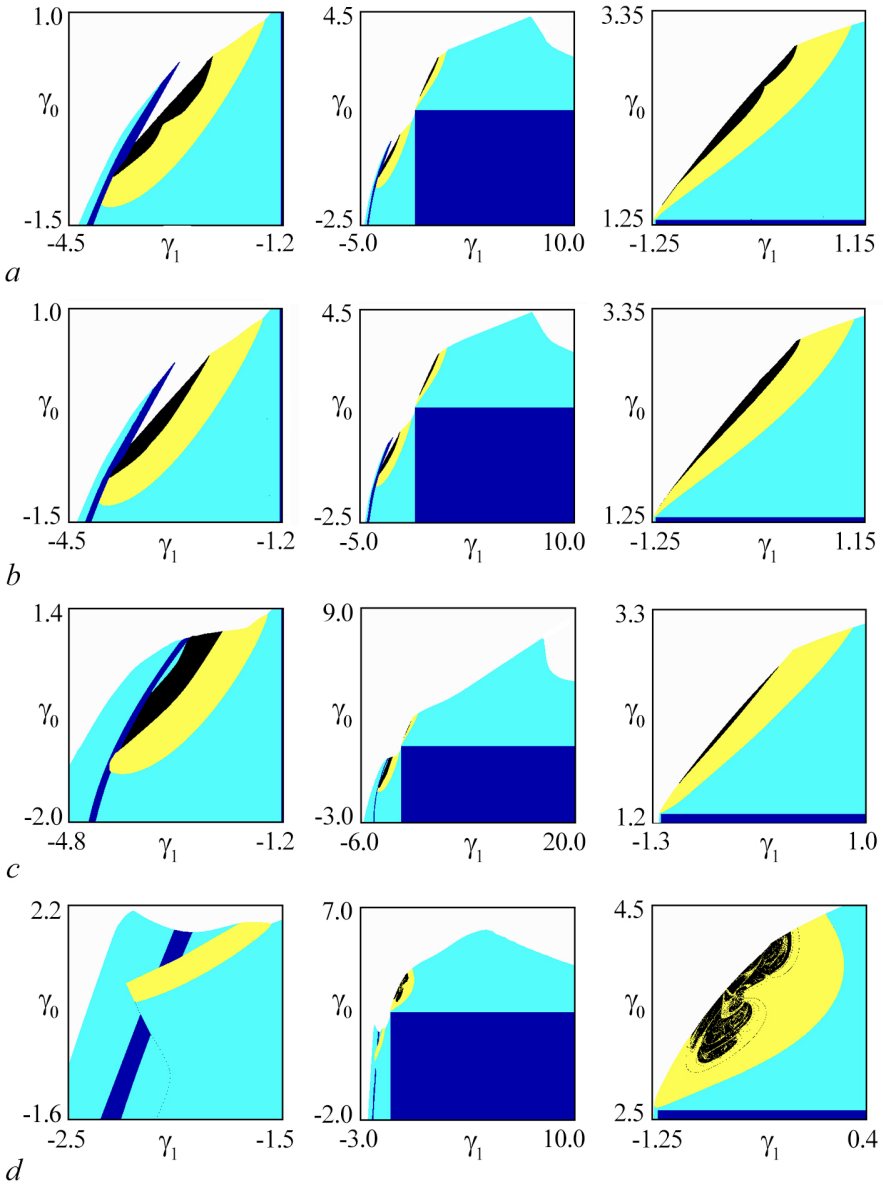

Fig 6. Charts of Lyapunov exponents of the system (17) and its magnified fragments at (γ_0, γ_1) parameter plane. *a* — $\omega_0 = 32\pi$, $\omega_1 = \omega_0 - 1$, $\mu = 8$, $\beta = 2$, $\alpha_0 = 1$, $\alpha_1 = 1$; *b* — $\omega_0 = 32\pi$, $\omega_1 = \omega_0 - 1$, $\mu = 8$, $\beta = 1.8$, $\alpha_0 = 1$, $\alpha_1 = 1$; *c* — $\omega_0 = 32\pi$, $\omega_1 = \omega_0 - 1$, $\mu = 16$, $\beta = 2$, $\alpha_0 = 1$, $\alpha_1 = 1$; *d* — $\omega_0 = 32\pi$, $\omega_1 = \omega_0 - 1$, $\mu = 8$, $\beta = 2$, $\alpha_0 = 0.5$, $\alpha_1 = 1$ (color online)

the ranges of variation of the generalized velocities of the oscillators are y_0, y_1 and generalized coordinates of the oscillators x_0, x_1 differ by an order of magnitude. Lyapunov exponents for this mode: $\Lambda_1 = 0.00000 \pm 0.00001$, $\Lambda_2 = -0.10586 \pm 0.00001$, $\Lambda_3 = -0.10588 \pm 0.00001$, $\Lambda_4 = -0.74386 \pm 0.00001$.

If we continue to increase the parameter γ_0 or decrease the parameter γ_1, then the limit cycle disappears and a two-frequency torus is born instead. At the same time, in the graphs of the dependence of Lyapunov exponents, two indicators, the first and second, become equal to zero, while the third and fourth remain negative (see Fig. 7). In addition, it is clear from the figure that in the region of existence of the torus, the graph of the third Lyapunov exponent has a form typical for systems with period doubling. Thus, it can be argued that in the system under consideration there is a sequence of torus doubling bifurcations, which leads to the emergence of a chaotic regime. In this case, the highest Lyapunov exponent becomes positive (see Fig. 7). The corresponding projections of the attractor onto the phase planes of the oscillators are presented in Fig. 8, *b*–*d*. Fig. 8, *b* shows projections of a torus of period one, and Fig. 8, *c* shows a torus of period two. The Lyapunov exponents for these modes are, respectively, $\Lambda_1 = 0.00000 \pm 0.00001$, $\Lambda_2 = -0.00000 \pm 0.00001$, $\Lambda_3 = -0.15592 \pm 0.00001$, $\Lambda_4 = -0.15593 \pm 0.00001$ and $\Lambda_1 = 0.00000 \pm \pm 0.00001$, $\Lambda_2 = -0.00000 \pm 0.00001$, $\Lambda_3 = -0.06971 \pm 0.00001$, $\Lambda_4 = -0.06973 \pm 0.00001$. And in Fig. 8, *d* the projections of a chaotic attractor are shown, the Lyapunov exponents of which have the values $\Lambda_1 = 0.09681 \pm 0.00001$, $\Lambda_2 = -0.00000 \pm 0.00001$, $\Lambda_3 = -0.00000 \pm 0.00001$,

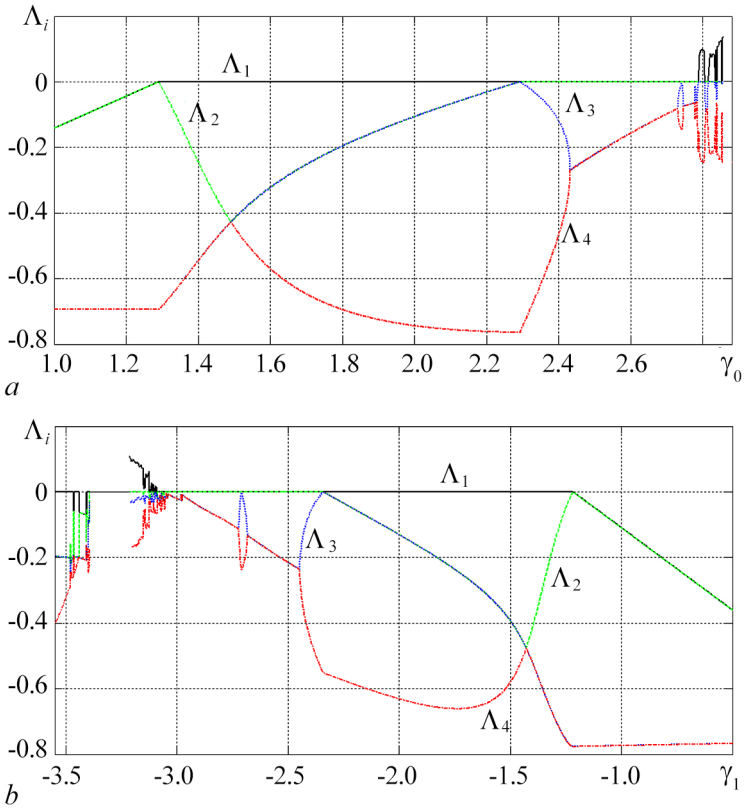

Fig 7. *a* — Graphs of Lyapunov exponents of the system (17) at the value of the parameter γ_0, $\gamma_1 = 0.2$. *b* — Graphs of Lyapunov exponents of the system (17) at the value of the parameter γ_1, $\gamma_0 = -0.3$. Other parameters are $\omega_0 = 32\pi$, $\omega_1 = \omega_0 - 1$, $\mu = 8$, $\beta = 2$, $\alpha_0 = 1$, $\alpha_1 = 1$. The gap in the graphs corresponds to the area where the trajectory go to infinity (color online)

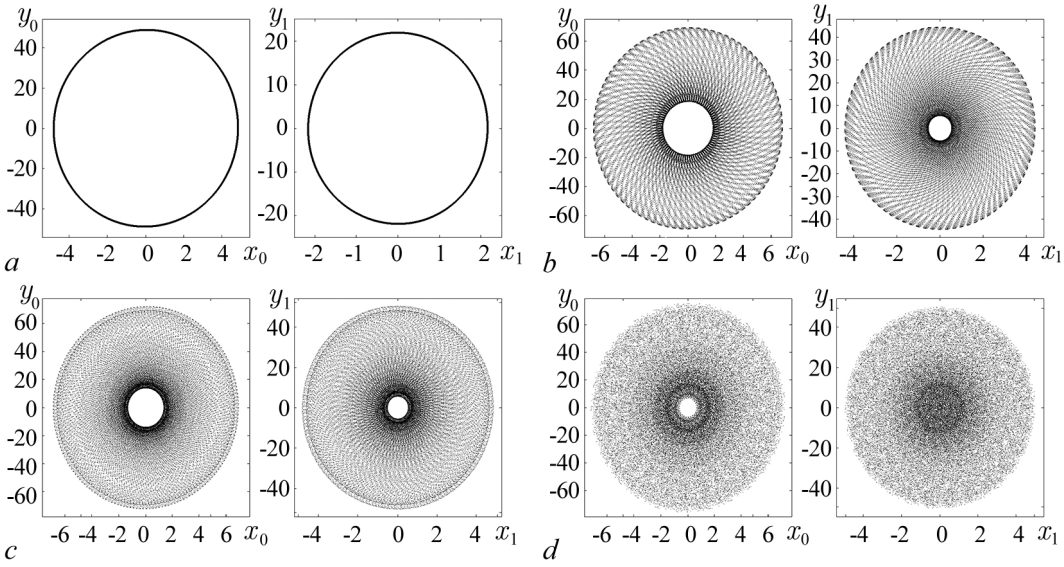

Fig 8. Projections of the attractors on the plane (x_0, y_0) and (x_1, y_1) of the system (17). *a* — The limit cycle, $\gamma_0 = 2.0$; *b* — the two-frequency period one torus, $\gamma_0 = 2.6$; *c* — the two-frequency period two torus, $\gamma_0 = 2.76$; *d* — the chaos, $\gamma_0 = 2.8$. Other parameters are $\omega_0 = 32\pi$, $\omega_1 = \omega_0 - 1$, $\mu = 8$, $\beta = 2$, $\alpha_0 = 1$, $\alpha_1 = 1$

$\Lambda_4 = -0.24215 \pm 0.00001$.

Now, just like in the previous section, we will study the influence of the parameters included in the equations of the system (17) on its dynamics. First, we will change the parameters characterizing the nonlinear interaction between the oscillators. The study showed that changing (either increasing or decreasing) the parameter β does not affect the dynamics of the system (17). The corresponding map of Lyapunov exponents, constructed for $\beta = 1.8$ (other parameters remained unchanged), is presented in Fig. 6, *b*. From its comparison with the map presented in Fig. 6, *a*, it is clear that they are almost identical. Changing the parameter μ leads to the fact that the regions of existence of the limit cycle, torus and chaos, located to the left of the region of the trivial equilibrium position, increase in size if the parameter μ increases. While the areas of the same regimes located above the area of the trivial equilibrium position do not change. This is clearly visible on the map of Lyapunov exponents of the system (17), constructed for $\mu = 16$ and presented in Fig. 6, *c*. If the parameter μ decreases, then all regions of existence of the limit cycle, torus and chaos, regardless of their location, will also decrease in size until they completely disappear.

Now consider the case $\alpha_1 > \alpha_0$. The corresponding map of Lyapunov system exponents (17), constructed for the values $\alpha_0 = 0.5$, $\alpha_1 = 1$, is presented in Fig. 6, *d*. In this case, the regions of existence of all regimes observed in the system increase significantly in size, and the boundary of the region of existence of the trivial equilibrium position shifts up and to the left. The configuration of the region of existence of the torus, located above the region of the trivial equilibrium position, resembles the structure of the "crossroad area", and within the region corresponding to the chaotic regime, regions corresponding to two-frequency tori have appeared. With the opposite ratio of the parameters $\alpha_{1,2}$, the regions of existence of all modes, except for the region of the trivial equilibrium position, will correspondingly decrease in size, and the boundary of the region of existence of the trivial equilibrium position shifts down and to the right.

And finally, let us consider what a change in frequency ω_0 (frequency of the fundamental

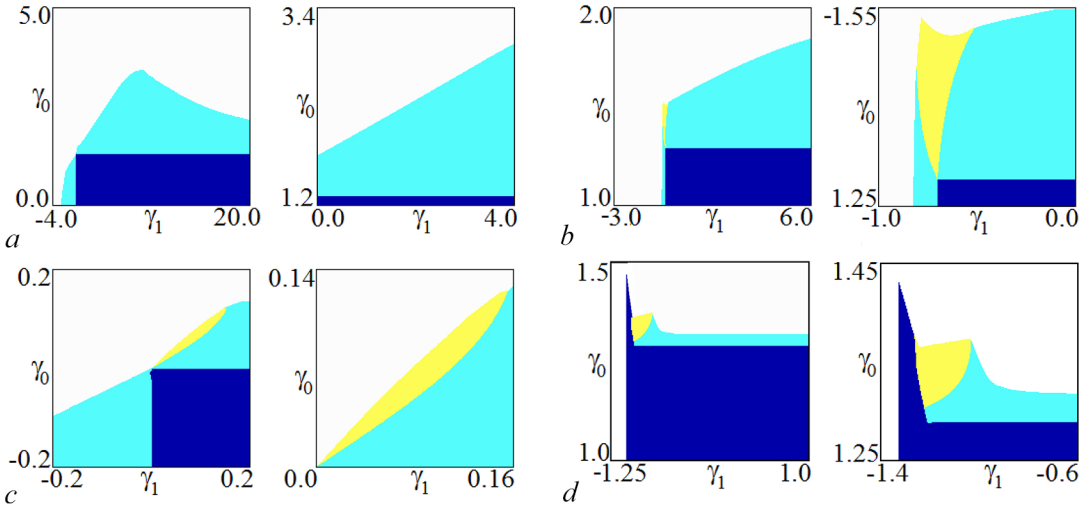

Fig 9. *a–c* — Charts of Lyapunov exponents of the system (17) and its magnified fragments at (γ_0, γ_1) parameter plane. *a* — $\omega_0 = 32\pi$, $\omega_1 = \omega_0 - 0.1$, $\mu = 8$, $\beta = 2$, $\alpha_0 = 1$, $\alpha_1 = 1$; *b* — $\omega_0 = 32\pi$, $\omega_1 = \omega_0 - 10$, $\mu = 8$, $\beta = 2$, $\alpha_0 = 1$, $\alpha_1 = 1$; *c* — $\omega_0 = 2\pi$, $\omega_1 = \omega_0 - 0.06$, $\mu = 8$, $\beta = 2$, $\alpha_0 = 1$, $\alpha_1 = 1$. *d* — Chart of Lyapunov exponents of the system (17) and it magnified fragment at (γ_0, γ_1) parameter plane. The chart plotted for the case when the interaction potential contains only resonant terms. $\omega_0 = 32\pi$, $\omega_1 = \omega_0 - 1$, $\mu = 8$, $\beta = 2$, $\alpha_0 = 1$, $\alpha_1 = 1$ (color online)

mode) and frequency deviation from resonance $\Delta\omega$ will lead to. Reducing the detuning from resonance $\Delta\omega$ while maintaining the frequency value ω_0, that is, the resonance condition is satisfied more strictly, leads to the disappearance of the regions of existence of two-frequency tori and chaos, while the regions of existence of the limit cycle and trivial the equilibrium positions do not change (Fig. 9, *a*). An increase in $\Delta\omega$ leads to the disappearance of the regions of existence of chaos and the two-frequency torus to the left of the region of the trivial equilibrium position and the region of the chaotic regime above the region of the trivial equilibrium position. The region of the torus located above the region of existence of the trivial equilibrium position is preserved, but changes its shape. Now it is similar in shape to the "Arnold's tongue", the base of which is located at the intersection point of the upper and left boundaries of the region of existence of the trivial equilibrium position (Fig. 9, *b*). A decrease in the frequency ω_0 (in this case, the deviation of the frequency from the resonance $\Delta\omega$ also decreases in proportion to the decrease in ω_0) leads to the complete disappearance of the region of existence of the chaotic mode and a significant decrease in the regions of existence of all others modes, with the exception of the region of the trivial equilibrium position (Fig. 9, *c*).

Finally, if in the equations of the system (17) in the expression for the interaction potential we leave only resonant terms, these are terms of the form x_0^3 and $3\mu x_0 x_1^2$ in the first equation and x_1^3 and $3\mu x_1 x_0^2$ in the second, then the change in the Lyapunov exponent map will be the same as when *changes*ω_0 and $\Delta\omega$ (Fig. 9, *d*). Namely, all areas of regular and chaotic regimes located to the left of the area of the trivial equilibrium position completely disappear. Above this region, one can observe only the regions of the limit cycle and the chaotic regime, which have significantly decreased in size.

In conclusion of this section, we note that a comparison of the map of dynamic regimes of the Rabinovich–Fabrikant model (2) (see Fig. 1, *b*) and maps of Lyapunov system exponents (17), primarily shown in Fig. 6, *a*, shows that they differ significantly from each other. This means that, unlike the Vyshkind-Rabinovich model, the Rabinovich-Fabrikant model cannot be used

as a three-dimensional real approximation of the original system of equations (17). At the same time, the question of at what stage of the derivation of the generalized Rabinovich-Fabrikant model the loss of accuracy occurred requires additional research.

Conclusion

In this work, systems of second-order ordinary differential equations with respect to real variables, constructed within the framework of Lagrange's mechanical formalism, are numerically studied, making it possible to describe the parametric interaction of two oscillators (oscillatory modes) in dissipative media with quadratic and cubic nonlinearities of general form. It was shown analytically that in the case of quadratic nonlinearity, the original system of second-order differential equations can be reduced to the three-dimensional real Vyshkind-Rabinovich model, and in the case of cubic nonlinearity, to the Rabinovich-Fabrikant model. For both systems under study, maps of Lyapunov exponents were constructed on the plane of frequency detuning from resonance — dissipation parameter of the second oscillator (fundamental mode) for the case of quadratic nonlinearity and on the plane of dissipation parameters of both oscillators for the case of cubic nonlinearity; dependence of the spectrum of Lyapunov exponents on the parameter that specifies the dissipation of oscillators; temporary realizations of generalized coordinates of oscillators and their amplitudes; projections of attractors onto phase planes of oscillators. The change in Lyapunov exponent maps was studied with variations in other parameters, such as parameters characterizing the nonlinear interaction of oscillators, oscillator frequencies, and frequency detuning from resonance. A comparison was also made of the results obtained for the systems under study with the known results for the Vyshkind-Rabinovich and Rabinovich-Fabrikant models.

The study of the first model (Section 1), obtained for the case of quadratic nonlinearity, showed that, firstly, only two types of modes are observed in the system. Namely, regular modes in the form of two-frequency tori of various periods and chaotic modes. Moreover, the transition to chaos occurs through a sequence of bifurcations of doubling the period of the tori. Secondly, at small values of the nonlinearity parameter in the system under consideration, a runaway to infinity is observed for the main mode and damping of oscillations for the satellite. When this parameter exceeds a threshold value in the system, oscillations become saturated. After which, changes in the parameters characterizing the nonlinear interaction between the oscillators have a weak effect, compared to other parameters, on the dynamics of the original system. But a change in the frequency of the first oscillator or the parameter characterizing its dissipation leads to rescaling of the maps of Lyapunov exponents. In this case, the boundary of transition from regular regimes to chaos shifts up or down depending on which parameter changes and how. For example, it will shift down if the dissipation parameter of the first oscillator decreases or if the frequency of the first oscillator increases. A comparison of the maps of Lyapunov exponents of the original system of differential equations with the map of dynamic regimes of the Vyshkind–Rabinovich model showed complete identity of their dynamics and allows us to conclude that the latter is an adequate three-dimensional approximation of the above system.

The study of the second model (Section 2), obtained for the case of cubic nonlinearity, showed that, unlike the first, it demonstrates a larger number of dynamic modes. Namely, the equilibrium position, the limit cycle, two-frequency tori of various periods, chaos. Moreover, such regimes as tori and chaos are observed only in the case of sufficiently large values of oscillator frequencies (about 100 normalized units) and not very large values of frequency detuning from resonance. An increase or decrease in the frequency detuning from resonance leads to their

disappearance, and only a trivial equilibrium position and a limit cycle of period one are observed in the system. Changing the parameters characterizing the nonlinear interaction between oscillators leads, in turn, to an increase or decrease in the areas of tori and chaos, depending on which parameter is changed and how. A comparison of the maps of Lyapunov exponents constructed for the original system of differential equations with the map of dynamic regimes of the Rabinovich-Fabrikant model showed their complete difference. This means that the Rabinovich-Fabrikant model cannot be used as a three-dimensional approximation of the above system. Moreover, taking into account only resonant terms in the equations of the original system does not improve the correspondence between the original system and the Rabinovich–Fabrikant model, but only leads to the complete disappearance of chaotic modes and a significant reduction in the regions of existence of two-frequency tori and the limit cycle. At the same time, the question of at what stage of the derivation of the Rabinovich-Fabrikant model the loss of accuracy occurred requires additional research.

References

1. Demidov VE, Kovschikov NG. Mechanism of occurrence and stochastization of self-modulation of intense spin waves. Technical Physics. 1999;69(8):100–103 (in Russian).
2. Romanenko DV. Chaotic microwave pulse train generation in self-oscillatory system based on a ferromagnetic film. Izvestiya VUZ. Applied Nonlinear Dynamics. 2012;20(1):67–74 (in Russian). DOI: 10.18500/0869-6632-2012-20-1-67-74.
3. Wersinger J-M, Finn JM, Ott E. Bifurcation and "strange" behavior in instability saturation by nonlinear three-wave mode coupling. The Physics of Fluids. 1980;23(6):1142–1154. DOI: 10.1063/1.863116.
4. Savage CM, Walls DF. Optical chaos in second-harmonic generation. Optica Acta: International Journal of Optics. 1983;30(5):557–561. DOI: 10.1080/713821254.
5. Lythe GD, Proctor MRE. Noise and slow-fast dynamics in a three-wave resonance problem. Physical Review E. 1993;47(5):3122–3127. DOI: 10.1103/PhysRevE.47.3122.
6. Kuznetsov SP. Parametric chaos generator operating on a varactor diode with the instability limitation decay mechanism. Technical Physics. 2016;61(3):436–445. DOI: 10.1134/S1063784216030129.
7. Pikovski AS, Rabinovich MI, Trakhtengerts VY. Appearance of chaos at decay saturation of parametric instability. Sov. Phys. JETP. 1978;47:715–719.
8. Vyshkind SY, Rabinovich MI. The phase stochastization mechanism and the structure of wave turbulence in dissipative media. Sov. Phys. JETP. 1976;44(2):292–299.
9. Rabinovich MI, Fabrikant AL. Stochastic self-modulation of waves in nonequilibrium media. Sov. Phys. JETP. 1979;50(2):311–317.
10. Kuznetsov SP, Turukina LV. Complex dynamics and chaos in electronic self-oscillator with saturation mechanism provided by parametric decay. Izvestiya VUZ. Applied Nonlinear Dynamics. 2018;26(1):33–47. DOI: 10.18500/0869-6632-2018-26-1-33-47.
11. Danca M-F, Chen G. Bifurcation and chaos in a complex model of dissipative medium. International Journal of Bifurcation and Chaos. 2004;14(10):3409–3447. DOI: 10.1142/S0218127404011430.
12. Danca M-F, Feckan M, Kuznetsov N, Chen G. Looking more closely at the Rabinovich–Fabrikant system. International Journal of Bifurcation and Chaos. 2016;26(2):1650038. DOI: 10.1142/S0218127416500383.
13. Liu Y, Yang Q, Pang G. A hyperchaotic system from the Rabinovich system. Journal of Computational and Applied Mathematics. 2010;234(1):101–113.

DOI: 10.1016/j.cam.2009.12.008.
14. Agrawal SK, Srivastava M, Das S. Synchronization between fractional-order Ravinovich–Fabrikant and Lotka–Volterra systems. Nonlinear Dynamics. 2012;69(4):2277–2288. DOI: 10.1007/s11071-012-0426-y.
15. Srivastava M, Agrawal SK, Vishal K, Das S. Chaos control of fractional order Rabinovich–Fabrikant system and synchronization between chaotic and chaos controlled fractional order Rabinovich–Fabrikant system. Applied Mathematical Modelling. 2014;38(13):3361–3372. DOI: 10.1016/j.apm.2013.11.054.
16. Danca M-F. Hidden transient chaotic attractors of Rabinovich–Fabrikant system. Nonlinear Dynamics. 2016;86(2):1263–1270. DOI: 10.1007/s11071-016-2962-3.
17. Danca M-F, Kuznetsov N, Chen G. Unusual dynamics and hidden attractors of the Rabinovich–Fabrikant system. Nonlinear Dynamics. 2017;88(1):791–805. DOI: 10.1007/s11071-016-3276-1.
18. Kuznetsov AP, Kuznetsov SP, Turukina LV. Complex dynamics and chaos in the Rabinovich–Fabrikant model. Izvestiya of Saratov University. Physics. 2019;19(1):4–18 (in Russian). DOI: 10.18500/1817-3020-2019-19-1-4-18.
19. Kuznetsov SP, Turukina LV. Generalized Rabinovich–Fabrikant system: equations and its dynamics. Izvestiya VUZ. Applied Nonlinear Dynamics. 2022;30(1):7–29. DOI: 10.18500/0869-6632-2022-30-1-7-29.
20. Turukina LV. Dynamics of the Rabinovich–Fabrikant system and its generalized model in the case of negative values of parameters that have the meaning of dissipation coefficients. Izvestiya VUZ. Applied Nonlinear Dynamics. 2022;30(6):685–701. DOI: 10.18500/0869-6632-003015.
21. Hocking LM, Stewartson K. On the nonlinear response of a marginally unstable plane parallel flow to a two-dimensional disturbance. Proc. R. Soc. Lond. A. 1972;326(1566):289–313. DOI: 10.1098/rspa.1972.0010.
22. Kuramoto Y, Yamada T. Turbulent state in chemical reactions. Progress of Theoretical Physics. 1976;56(2):679–681. DOI: 10.1143/PTP.56.679.
23. Kuznetsov AP, Sataev IR, Tyuryukina LV. Synchronization of quasi-periodic oscillations in coupled phase oscillators. Technical Physics Letters. 2010;36(5):478–481. DOI: 10.1134/S1063785010050263.
24. Pazó D, Sánchez E, Matías MA. Transition to high-dimensional chaos through quasiperiodic motion. International Journal of Bifurcation and Chaos. 2001;11(10):2683–2688. DOI: 10.1142/S0218127401003747.
25. Kuznetsov AP, Sataev IR, Turukina LV. Regional structure of two- and three-frequency regimes in a model of four phase oscillators. International Journal of Bifurcation and Chaos. 2022;32(3):2230008. DOI: 10.1142/S0218127422300087.
26. Kuznetsov SP. Dynamical Chaos. Moscow: Fizmatlit; 2006. 356 p. (in Russian).